# Non-Specular Reflectance in the Extreme Ultraviolet

**Quintin Nethercott, Cody Petrie, R. Steven Turley**

Brigham Young University

## Abstract

*Surface roughness is critical in extreme ultraviolet (EUV) optics because the short wavelengths make optics much more sensitive to variations in surface height. We measured the non-specular reflection from two chrome samples and fit that data to a model in order to characterize their surface features. As a result we have improved our ability to characterize surface roughness in the extreme ultraviolet by utilizing non-specular reflectance to complement and improve other methods for characterizing surface roughness such as atomic force microscopy (AFM) and electron microscopy. From the analysis of these measurements we are able to determine the surface roughness height of our sample to be 1.1 ± 0.2 μm. With more work we will be able to determine surface characteristics better than AFM and electron microscopy.*

# 1. Introduction and Background

Our current method of characterizing roughness using atomic force microscopy (AFM) is limited by our tips to a resolution of about 3 nanometers. Because of how our thin films are fabricated, we don't expect electron microscopy to be any more accurate than this. We hope to provide a new and more efficient way of measuring deviations in surface height based on non-specular measurements. The purpose of this paper is to provide a proof of principle showing that we can determine surface features based on non-specular reflection. To establish the proof of principle we used geometric optics because the size of the sample roughness was much greater than the wavelength of light. Geometrical optics is explained in more detail in section 3.1. For our normal samples the surface features have sizes comparable to the wavelength of the incident light. Analyzing non-specular reflection from such surfaces would require more careful calculations which are described by Greg Hart [1].

## 1.1 Non-Specular Reflection

Specular reflection occurs when light reflects from a surface at the same angle as the incident beam, obeying Snell's Law. Geometrical optics treats light as rays, allowing one to trace the propagation of light as illustrated in Figure 1. However, when the surface is non-planar the reflected light will scatter at different angles. This is called non-specular reflection and is illustrated in Figure 2.

The intensity of the light at a given angle is proportional to the density of rays at that angle. By measuring the intensity at the non-specular angles we hope to be able to quantify the noise height of different samples.

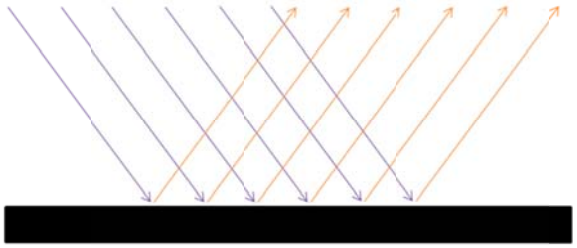

*Figure 1: Specular reflection, the reflected beams reflect at the same angle that they were incident to the surface.*

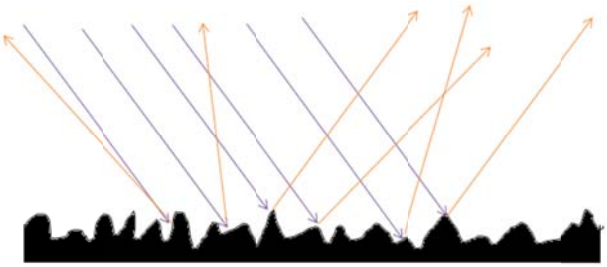

*Figure 2: Non-Specular reflection, the reflected beams reflect at angles other than the angle of incidence.*

## 1.2 EUV

For our purposes we define EUV to be between 1 and 60 nm on the electromagnetic spectrum. One difficulty in using EUV arises because EUV radiation is absorbed very quickly in air. As a result we do all of our measurements under vacuum. Though the EUV is difficult to study it is a useful tool in many fields. Photolithography is the most common process by which computer chips are made. Because of diffraction, the size of the computer chips is limited by the wavelength of light used. Currently visible and UV light can be used in photolithography. Using EUV light in photolithography would enable us to make even smaller computer chips. Another application of EUV light exists in astrophysics. Because different wavelengths illuminate different features of astrophysical objects, EUV observations are an important tool for learning about these objects. In particular, the EUV can be used to study transitions from singly ionized He and blackbody radiation from stellar interiors. Other applications of the EUV exist in medicine, microscopy, and plasma diagnostics.

Since the wavelength of EUV light is short compared to the characteristic features size on our chrome samples we used geometrical optics to analyze our reflection data. We will eventually be able to detect surface roughness on a scale comparable to the wavelength of EUV

light. However, in this paper we are using a simplified calculation to prove that this will be possible. We hope to eventually improve our current methods of characterizing surface roughness through atomic force microscopy and electron microscopy.

## 2. Calculating Non-Specular Reflection

Currently we have measured reflection data from two black chrome samples provided to us by Lawrence Livermore National Laboratory. Their project is sensitive to EUV light and needed to minimize non-specular reflection from their surfaces [2]. The samples are different in surface roughness and were part of a project to compare surfacing techniques that would minimize non-specular reflection in the EUV. The measurements we will be discussing are from a sample that shows grooves that are approximately 18 μm in diameter and have additional roughness with a dominant spatial frequency of 0.3 to 0.4 $\mu m^{-1}$.

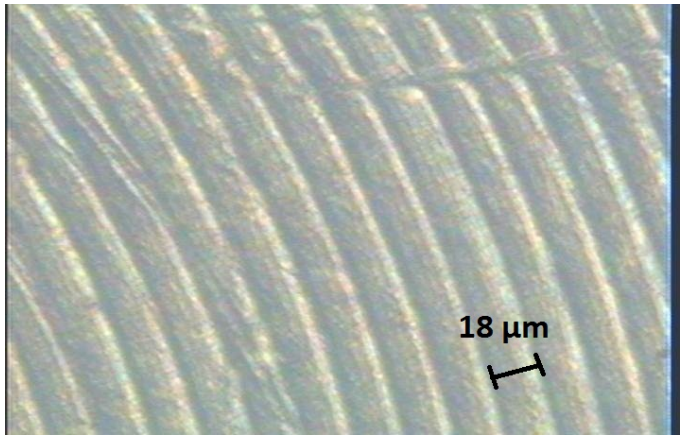


*Figure 3: This is an image of our chrome sample taken under a visible microscope to show the 18 μm grooves up close.*

We used a vacuum chamber reflectometer to measure the non-specular reflection of EUV light. To do this we created a monochromatic beam of EUV light using a hollow cathode light source, which uses a He plasma and a grazing-incidence monochromator. Our hollow cathode was designed after the source described in [3]. This light is then directed into our vacuum

chamber through a pinhole that is 0.3 ± 0.1 mm in diameter which defines the beam. There is a sample stage in the center of the chamber 17.4 ± 0.2 cm from the pinhole that can be rotated as well as moved in all three directions. We took our measurements using a detector 15.3 ± 0.2 cm from the sample stage that can be rotated around the edges of the chamber. The detector that we used is a channel electron multiplier and can detect single photons as they enter the entry aperture of 3.2 ± 0.5 mm diameter.

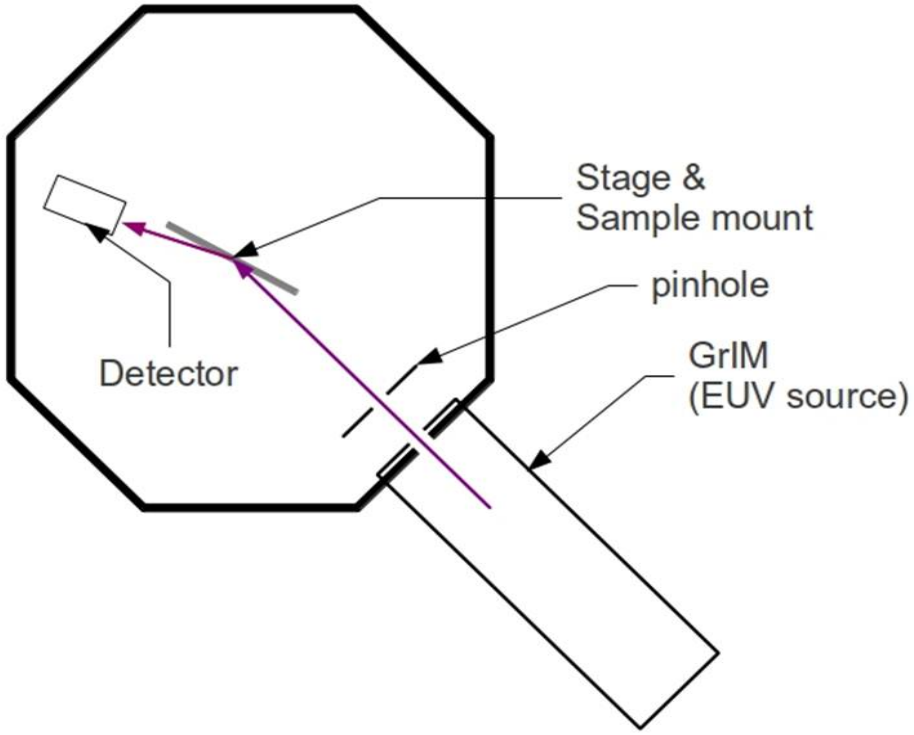


*Figure 4: This is a depiction of our vacuum chamber showing the detector, stage mount, pinhole and hollow cathode with grazing-incidence monochromator.*

We took several measurements in order to calculate the reflection from the sample as a function of angle. We measured the incident beam profile in order to normalize the reflection and compare the reflection measurements, the background noise that is in the chamber, and the random noise, or dark counts, that we got from our detector. To measure the beam profile we moved the sample stage out of the path of the beam and scanned the detector across the beam to

see the number of incident photons. The background measurement was taken when there was a beam in the chamber, but it was not being reflected from the sample. The detector was scanned across the angles that we measured for the reflection to pick up the background EUV light that was in the chamber. The dark counts were measured by running the detector when there was no beam in the chamber. A typical dark count measurement from our detector is around 1 count per second. Finally, the reflection measurement was taken by scanning the detector from 0 to 90° where 0° is the specular angle of reflection. Our detector has an angular acceptance of 1.2 ± 0.8° based on the size of the entry aperture and the distance from the sample to the detector.

## 3. Analysis

To calculate the reflection as a percentage of the incident beam we took into account the fact that the light passes through a circular hole before entering the detector, and normalized it with the background, dark counts, and incident beam.

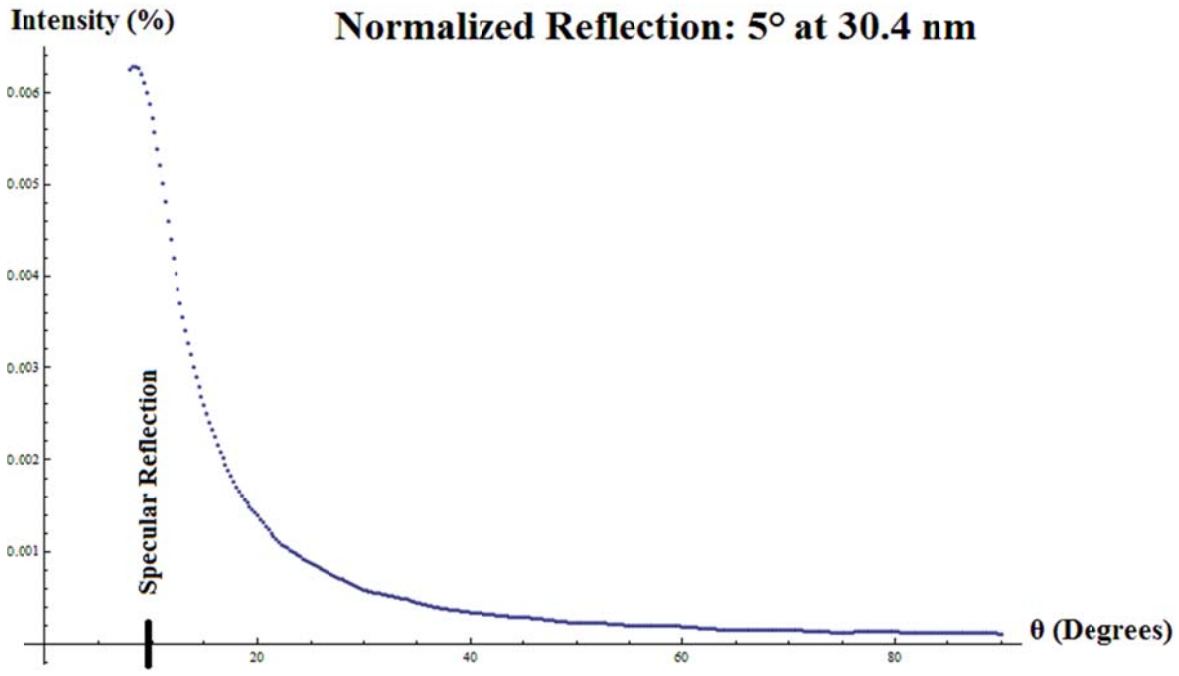


*Figure 5: Reflection data once normalization process has been completed. The y-axis is the percent intensity that is reflected at the given angle. In this case the incident angle was 5°.*

Since the light that we measured was the light from the incident beam that passes through a vertical slit and a circular aperture we treated our measurements as a convolution of the two shapes. A convolution is a combination of the beam exiting a slit and the light through the circular aperture and its equation is given by equation (1) where $[f * g](\theta)$ is the convolution of $f$ and $g$.

$$[f * g](\theta) = \int_{-\pi}^{\pi} f(\varphi) g(\theta - \varphi) d\varphi \quad (1)$$

To then determine what the incident beam looked like before smearing we performed a deconvolution of our measurement with the function we calculated for a slit of light passing through a circular aperture. We did this by utilizing the convolution theorem [4]. If $\hat{f}$ is the Fourier transform of $f$, then the convolution theorem states.

$$\widehat{(f * g)} = \hat{f}\, \hat{g} \quad (2)$$

Therefore if the smeared beam is $h(\theta) = f * g$ then $\hat{h} = \hat{f}\, \hat{g}$ or $\hat{g} = \frac{\hat{h}}{\hat{f}}$. We were then able to solve for the incident beam $g$ by performing an inverse Fourier transform of $\frac{\hat{h}}{\hat{f}}$.

We integrated the measurement for our incident beam to get the number of incident photons. Where the background was statistically significant it was also subtracted out. We then divided the reflection calculation by this to normalize it and get a percentage reflection as a function of angle.

## 3.1 Modeling Surfaces and Surface Characteristics

In order to show that we are able to learn more about the surface features by looking at the reflectance data we have modeled different surfaces, and varied some surface parameters in order to match a calculated reflection with our measurements. Since the surface features on the sample are much larger than the wavelength of our light we used geometrical optics to calculate

the reflection for our model surfaces. Geometrical optics is the process of tracing a ray of light as it reflects from a surface. First one assumes that the surface is locally planar. With this assumption one can trace a ray of light using Snell's Law to determine the angle of reflection.

We explored four different models in our calculations. The first model used a cubic spline to interpolation between a Gaussian distribution of points within a set height and length (Figure 6). The cutoff spatial frequency in this model was determined by the spacing between random surface heights. However, to better match the measurements taken on thin films by Alex Rockwood in his senior thesis we decided to try a filtered model [5]. To make a "filtered" distribution we took a Gaussian model, whose points were more closely spaced than in the previous model, and cut out the high frequency noise (Figure 7). We did this by doing a Fourier transform on the Gaussian model, multiplying it by a Gaussian function, and then doing the inverse Fourier transform. The third model we used was a $\sin^2$ function (Figure 8) that more closely represented the image we saw of our sample, but had no noise on top of the $\sin^2$ function. The last model was a $\sin^2$ function that has Gaussian noise on top of the $\sin^2$ (Figure 9), which most closely resembled the image of our sample.

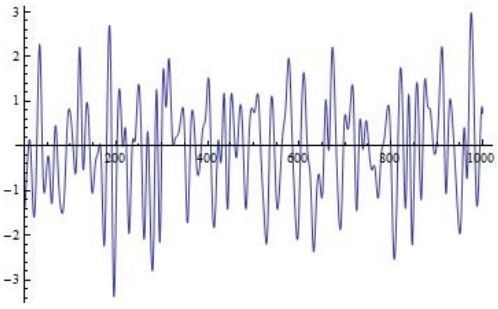


*Figure 6: Gaussian surface, made by an interpolation between a random Gaussian set of points.*

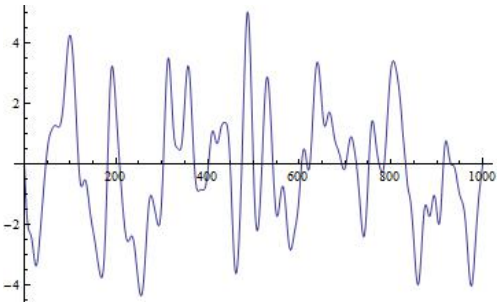


*Figure 7: Filtered Gaussian, made by filtering out high frequency variations in the Gaussian surface.*

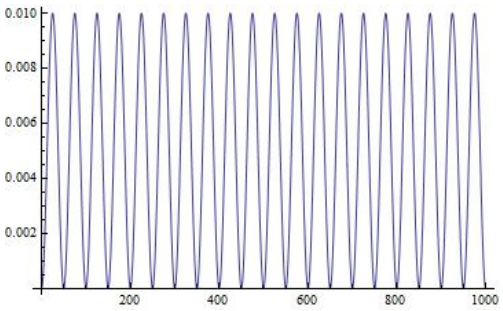


*Figure 8: Sin$^2$ surface, this surface does not include any noise on top of the sin$^2$.*

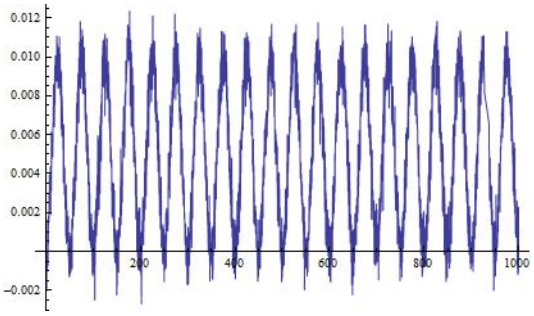


*Figure 9: Sin$^2$ with noise, this is made by putting noise on top of the sin$^2$ surface.*

We chose to explore a periodic surface because the image we took of the surface appears periodic. However, as seen in Figure 10 the reflection calculation for a sin$^2$ function looked nothing like what we saw in the data so we quickly dismissed this surface and conclude that it is the noise and smaller surface features that contribute most to the reflection measurements.

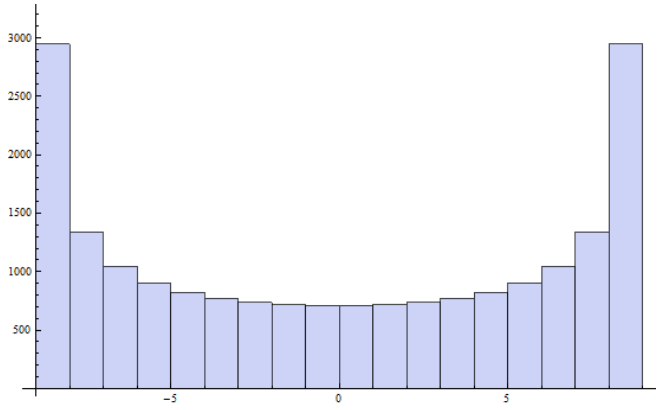


*Figure 10: Reflection data from sin$^2$ surface. This clearly does not match the reflection data that we see in Figure 5.*

We then looked at the effects that varying the parameters on our filtered Gaussian model had. We varied the number of points, the length of the surface, the height of the noise, and the standard deviation of our Gaussian cut-off. As we increased the number of points that made up our surface we were able to increase the height of the reflection peaks intensity however the

general shape of the data stayed the same. As we increased the length of the surface the peak height stayed the same but the peak became narrower. As we increased the height of the noise we noticed that the peak was most narrow at a specific value and then became less defined (more spread out) as you moved away from that value. The spread of values increased as the height of the noise increased. When the cutoff frequency was too low the shape of the reflectance data was fairly random however at a specific value it began to take a Gaussian shape. As the cutoff frequency was increased the peak spread out and became less defined and the range of values increased. The effect on our fitting data as we changed the noise height is illustrated in Figures 11 and 12.

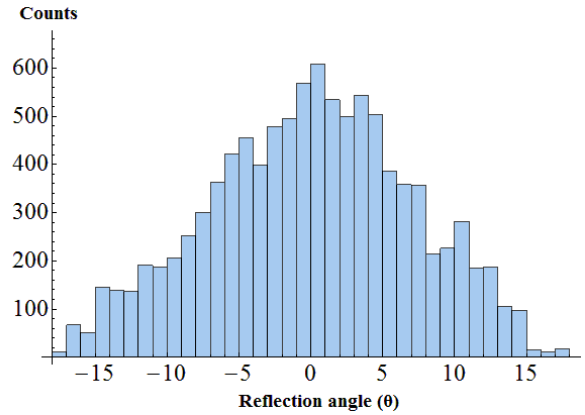


*Figure 11: Fitting data when noise height is set to 0.32 µm.*

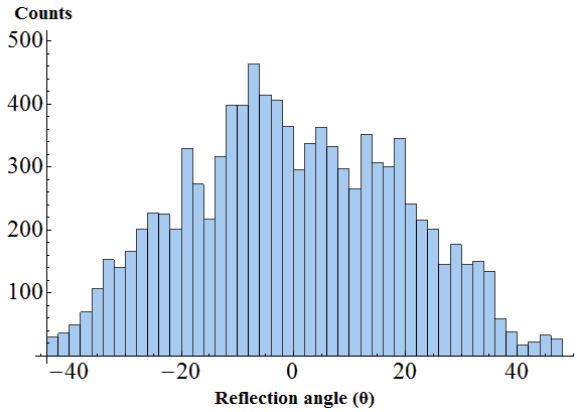


*Figure 12: Fitting data when noise height is raised to 0.96 µm. Notice how the peak decreased and the distribution of angles broadened.*

We were able to show that we can vary the parameters and match the histogram of our calculated reflectance with the profile of our reflectance measurement, as you can see in Figures 13, 14 and 15. This proves that we are able to learn about the surface characteristics of samples by analyzing the non-specular reflection.

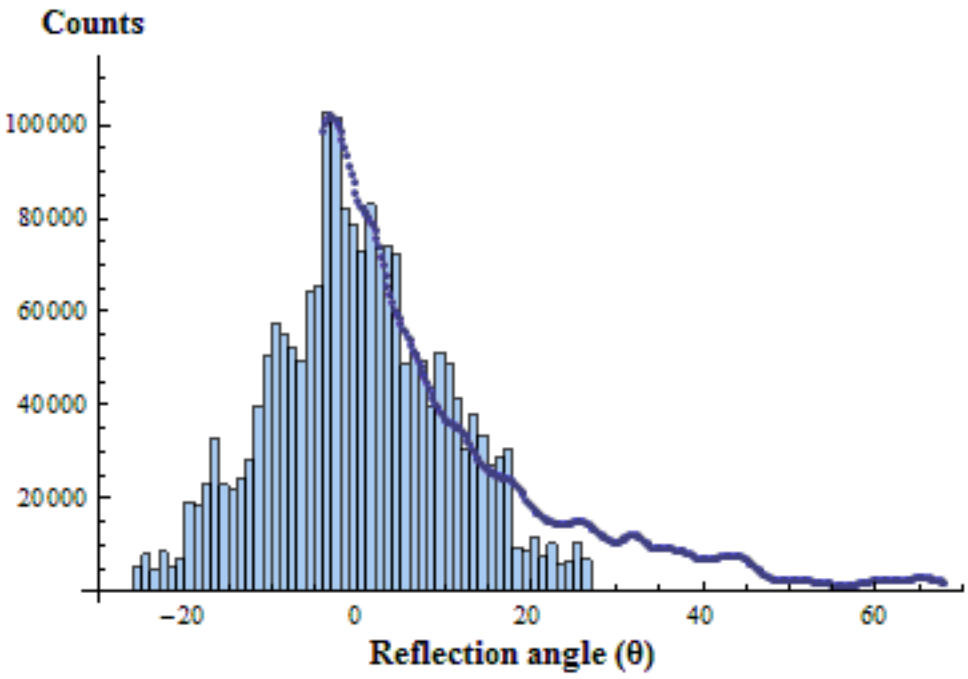


*Figure 13: Sample reflection data fitting. This is the reflection data taken from the chrome sample at 10° from 25.6 nm light. The bold blue cure is the actual reflection data and the blue histogram is the reflection data from our fitting model.*

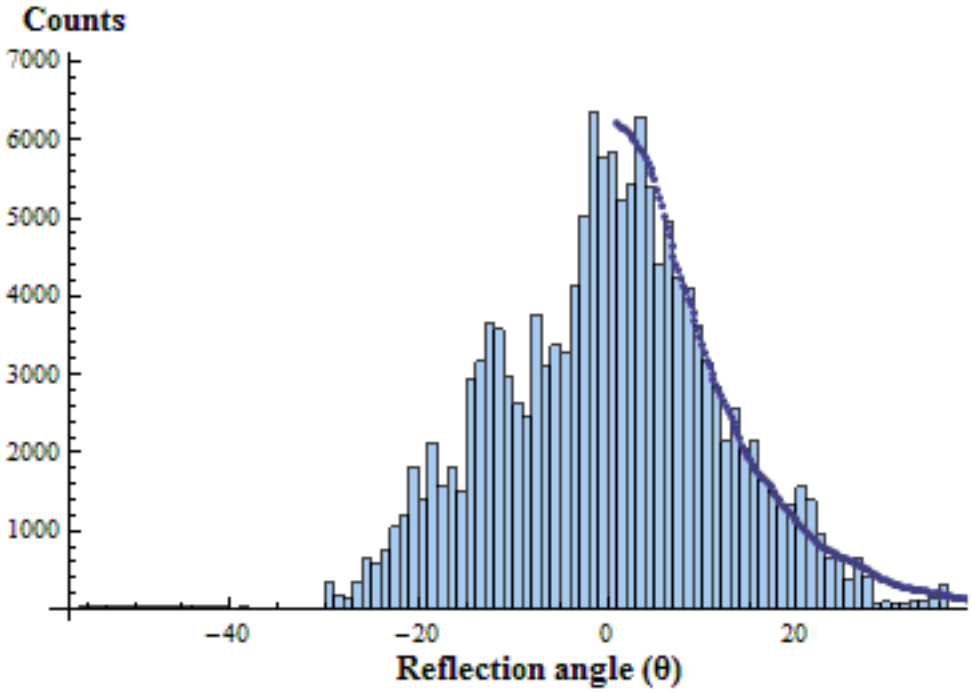


*Figure 14: This is the reflection data taken from the chrome sample at 10° from 30.4 nm light and fitted to the reflection curve from a modeled surface.*

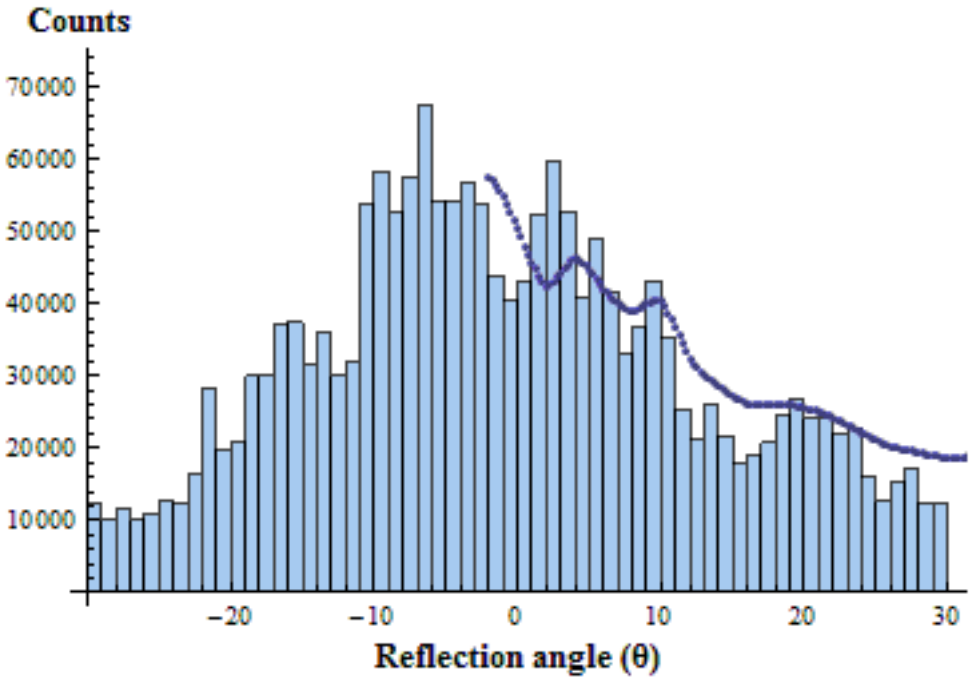


*Figure 15: This is the reflection data taken from the chrome sample at 20° from 30.4 nm light and fitted to the reflection curve from a modeled surface.*

## 4. Conclusion

We have measured the non-specular reflection from chrome samples and have been able to fit the reflection data to the reflection data from model surfaces. Based on these models we have determined that surfaces can be characterized based on non-specular reflection. We were able to calculate the average noise height to of chrome samples to within 1.1 ± 0.2 μm. While the resolution of this method was sensitive to the roughness on the 1.1 μm scale we hope to eventually achieve better resolution than AFM. To do this we will need to use the method described by Greg Hart [1]. We determined that the non-specular reflection was more sensitive to smaller variations on surface height than to the much larger $\sin^2$ variations. This was

determined since the fitting reflection data from the $\sin^2$ function (Figure 10) alone looked nothing like our reflection data. Characterizing surface features based on non-specular reflection will allow for the design of more efficient and accurate optical equipment in the EUV.

## 5. Acknowledgements

We acknowledge and thank James Vaterlaus and the many other students who have worked on this project collecting and analyzing reflection data. We acknowledge John Ellsworth from the Physics Department of Brigham Young University for working with us to keep our equipment running. Lawrence Livermore National Laboratory provided the chrome samples that were studied. This research was funded by the REU program at Brigham Young University under contract # R0112128 and by the Physics Department of Brigham Young University.

## References

[1] Gregory Hart and R. Steven Turley, "The Effect of Surface Roughness on Reflected Intensity," Utah Academy of Sciences, Arts, and Letters, 2012.

[2] M. P. Perkins, T. L. Houck, A. R. Marquez, and G.E Vogtlin, "Simulations for Initiation of Vacuum Insulator Flashover," Power Modulator and High Voltage Conference (IPMHVC), 2010 IEEE International, 727-730.

[3] F. Paresce, S. Kumar, and C. S. Bowyer, "Continuous Discharge Line Source for the Extreme Ultraviolet," *Applied Optics*, v. 10, p. 1904, 1971.

[4] William H. Press, Saul A. Teukolsky, William T. Vetterling, and Brian P. Flannery, "Numerical Recipes in C," Cambridge University Press, 1992.

[5] Alex Rockwood, "Modeled Roughness of a Sputtered Surface and its Effects on Extreme Ultraviolet Reflection," Senior Thesis Brigham Young University, 2011.